

Glucose transporter GLUT1 influences *Plasmodium berghei* infection in *Anopheles stephensi*

Mengfei Wang

Fudan University

Jingwen Wang (✉ jingwenwang@fudan.edu.cn)

Fudan University <https://orcid.org/0000-0002-6794-2604>

Research

Keywords: Anopheles stephensi, Plasmodium berghei, Asteglut1, transcriptome analysis

Posted Date: March 24th, 2020

DOI: <https://doi.org/10.21203/rs.2.22068/v2>

License:   This work is licensed under a Creative Commons Attribution 4.0 International License.

[Read Full License](#)

Version of Record: A version of this preprint was published at Parasites & Vectors on June 5th, 2020. See the published version at <https://doi.org/10.1186/s13071-020-04155-6>.

Abstract

Background: Sugar feeding provides energy for mosquitoes. Facilitated glucose transporters (GLUTs) are responsible for the uptake of glucose in animals. However, the knowledge of GLUTs function in *Anopheles* mosquito is limited.

Methods: Phylogenetic analysis of GLUTs in *Anopheles stephensi* (Asteglut) was performed by the maximum likelihood and Bayesian method. The spatial and temporal expression patterns of the four Astegluts were analyzed by qPCR. The function of Asteglut1 was examined using a dsRNA-mediated RNA interference method. Transcriptome analysis was used to investigate the global influence of Asteglut1 on mosquito physiology.

Results: We identified 4 glut genes, Asteglut1, Asteglutx, Asteglut3 and Asteglut4 in *An. stephensi*. Asteglut1, Asteglut3 and Asteglut4 were mainly expressed in the midgut. *Plasmodium berghei* infection differentially regulated the expression of Astegluts with significant downregulation of Asteglut1 and Asteglut4, while upregulation of Asteglutx. Only knocking down Asteglut1 significantly increased the susceptibility of *An. stephensi* to *Plasmodium berghei* infection. This might be due to the accumulation of glucose prior to blood feeding in dsAsteglut1-treated mosquitoes. Our transcriptome analysis revealed that knockdown of Asteglut1 differentially regulated expression of genes associated with multiple functional clusters including detoxification and immunity. The dysregulation of multiple pathways might contribute to the increased *P. berghei* infection.

Conclusions: Our study shows that Asteglut1 is essential in defense against *P. berghei* in *An. stephensi*. The regulation of Asteglut1 on vector competence might through modulating multiple biological processes, including detoxification and immunity.

Background

Anopheles mosquitoes are the primary vectors of human malaria that kill over 450,000 people annually [1]. To transmit between mammalian hosts, malaria parasites have to complete multiple development processes in mosquito including gametogenesis, fertilization, zygote-to-ookinete conversion and oocyst formation [2]. During this process, complicated interactions between *Anopheles* mosquitoes and *Plasmodium* parasites occur [3]. The nutrient availability is one of the key factors that determine the infection outcome [4, 5]. Sugar is a key energy resource that influences survival and fecundity of mosquitoes [6]. It also affects the vector competence [6, 7, 8, 9, 10]. Trehalose, the main circulating sugar, is a nonreducing disaccharide composed of two glucose molecules linked by an α - α -1,1-glycosidic bond. It enters cell metabolism after catabolized into glucose [11, 12]. Trehalose transporter AgTreT1 is responsible for the transportation of trehalose from fat body to hemolymph [13]. Knocking down Tret1 leads to the reduction of hemolymph trehalose and inhibition of *Plasmodium falciparum* infection [13].

Glucose is the primary source of energy for both mosquitoes and *Plasmodium* [14, 15]. During the blood stage and liver stage of malaria infection, *Plasmodium* parasites increase the absorption of glucose in

host cells by enhancing the translocation of GLUT1 to the cell membrane [16, 17]. Then these parasites scavenger host glucose by their facilitative hexose transporter (PfHT) [18]. However, the interactions of glucose metabolism between *Anopheles* mosquitoes and *Plasmodium* are still unclear. Only one glucose transporter, *AGAP007752*, is reported to be involved in facilitating *Plasmodium* sporozoites infection in *Anopheles gambiae*, and its knockdown decreased the number of sporozoites in mosquito salivary glands. [19, 20, 21].

In this study, we identified four *Asteglut* genes in *An. stephensi*. RNAi-mediated silencing of *Asteglut1* specifically increased *P. berghei* infection and significantly elevated the glucose level in mosquito midgut prior to blood feeding. The accumulation of midgut glucose might modulate multiple biological processes, including detoxification and immunity, which in turn increased parasite infection.

Methods

Mosquito rearing and maintenance

Anopheles stephensi (strain Hor) was reared at 28°C, 80% relative humidity. Adults were maintained on 2% sucrose solution. Adult female mosquitoes were fed on BALB/c mice for a blood meal.

Plasmodium berghei infection

Plasmodium berghei (ANKA strain) parasites expressing GFP constitutively were maintained by passing through BALB/c mice by mosquito biting [22, 23]. When parasitemia of *P. berghei* infected mice rises to 3%~6%, mosquitoes starved overnight were allowed to feed on it for 15 minutes. Engorged mosquitoes were maintained at 20 °C and unengorged ones were removed 24 hours post blood meal. Midguts were dissected and oocyst number were counted under the fluorescence microscope 8 days post infection. For melanization assay, midguts were dissected 8 days post infection and fixed in 4% formaldehyde for 30 min. Numbers of fluorescent oocysts and melanized ookinetes were visualized under a Nikon fluorescence microscope. Pictures were taken using a Nikon confocal microscope.

Phylogenetic analysis

Sequences were aligned using the default settings in MEGA X software [24]. Phylogenetic tree was constructed using the Maximum Likelihood method based on a bootstrapping method with 1000 replicate. The tree was drawn to scale, with branch lengths measured in the number of substitutions per site. Twenty five protein sequences were included in Phylogenetic analysis. The sequences obtained from database were: 4 glucose transporters of *Anopheles stephensi*, (ASTE005839, ASTE003001, ASTE006385 and ASTE008063), 4 sugar transporters of *Anopheles gambiae* (AGAP007340, AGAP005238, AGAP007752 and AGAP003020), 4 sugar transporters of *Aedes aegypti* (AAEL020018, AAEL006264, AAEL007136 and AAEL010868), 4 sugar transporters of *Drosophila melanogaster* GLUT1

(FBpp0305693), SUT-1 (FBpp0087855), MFST (FBpp0077268) and MFST (FBpp0075675), and 13 glucose transporters of *Homo sapiens*, GLUT1 (NP_006507.2), GLUT2 (XP_011511389.1), GLUT3 (NP_008862.1), GLUT4 (AAI13593.1), GLUT5 (NP_001315548.1), GLUT6 (XP_016869725.1), GLUT7 (XP_011539126.1), GLUT8 (XP_011516904.1), GLUT9 (XP_011512158.1), GLUT10 (XP_011527362.1), GLUT11 (NP_110434.3), GLUT12 (XP_006715412.1) and GLUT14 (XP_024304616.1).

RNA interference

The *Asteglut* genes were amplified by the corresponding primers. *Asteglut1*, F:5'-ACA GTA CAA CAG GTG AAG GAA GAG-3' and R: 5'-GTA ATC CTA CGG TCA CAG CCA AT-3', *Asteglutx*, F:5'-GCT GTC AGG AAT CAA TGC CGT CTT-3' and R:5'-CGC CAC CTC CGT TAC CTC TTG-3'; *Asteglut3*, F:5'- GCA TTG TTG AGC CAG CCC AAA-3' and R:5'-CTG CCT CGC CTA GTC CAT TCC-3'; *Asteglut4*, F:5'- CCA GAT TGC CGA ACC GAT GAC-3' and R:5'-TCA CCG TGC TCA CCG ATG AT-3'. Primers with T7 promoter sequence (TAATACGACTCACTATAGGG) were used to generate templates for double-stranded RNA (dsRNA). The dsRNAs were synthesized using the MEGAscript RNA kit (Ambio, Invitrogen, Shanghai, China). The plasmid eGFP (BD Biosciences, Shanghai, China) was used as controls. Four days old mosquitoes were injected with 69 nl dsRNA (4 µg/µl) using a nanoject II microinjector (Drummond, City, USA, America). The dsRNA-treated mosquitoes were collected two days post-treatment and knocking down efficiency was verified by qPCR as previously described [25].

RNA isolation, cDNA synthesis and quantitative PCR (qPCR)

Total RNA was extracted from mosquitoes using TRIzol reagent (Sigma-Aldrich, Shanghai, China) according to the manufacturer's protocol. One µg of total RNA was used to synthesize cDNA using 5' All-in-One MasterMix (AccuRT Genomic DNA Removal Kit, ABM, Shanghai, China). The qPCR was performed by Roche LightCycler 96 Real Time PCR Detection System using SYBR Green qPCR Master Mix (Biomake, Shanghai, China) according to a previously described protocol [25]. The data were processed and analyzed with LightCycler 96 software. Ribosomal gene *s7* was used as the internal reference gene.

Sugar measurement

The glucose and trehalose level in the mosquito hemolymph and midgut were examined as described [13, 26]. Briefly, 30 µl hemolymph was collected from 10 mosquitoes. Ten midguts were pooled together and homogenized in 30 µl PBS buffer. 30 µl of midgut homogenates and hemolymph, respectively, were used for glucose and trehalose measurement. Ten µl e was used to measure the glucose level with the Glucose Kit (Megazyme; K-GLUC, Bray, Ireland). Another ten µl was treated with trehalase enzyme (Megazyme; K-TREH, Bray, Ireland), and then examined for glucose concentration. Trehalose concentration was calculated as described [13]. The remaining 10 µl was used for genomic DNA extraction and

quantification [27]. The concentration of glucose and trehalose were normalized to the amount of genomic DNA, respectively.

RNA Sequencing

Mosquitoes treated with dsAsteglut1 and dsGFP 24 hours post infectious blood meal were collected for RNA sequencing. Four mosquitoes were pooled for one sample and three biological replicates were used from each treatment. Total RNA was extracted using TRIzol® Reagent according the manufacturer's instructions (Sigma-Aldrich, Shanghai, China) and sent to Majorbio (Shanghai, China) for library construction and sequencing using Illumina HiSeq 10. Clean data were aligned to the reference genome AsteS1.6 (<https://www.vectorbase.org/organisms/anopheles-stephensi>). To identify DEGs (differential expression genes) between two groups, the expression level of each transcript was calculated according to the fragments per kilobase of exon per million mapped reads (FPKM) method [28]. R statistical package software EdgeR (Empirical analysis of Digital Gene Expression in R, <http://www.bioconductor.org/packages/2.12/bioc/html/edgeR.html>) was used for differential expression analysis[29]. GO functional enrichment were carried out by Goatoools (<https://github.com/tanghaibao/Goatoools>). Heat map and Venn map are performed by TBtools software (v0.66831, <https://github.com/CJ-Chen/TBtools-Manual>)[30]. Pie chart, scatter chart and histogram were performed by GraphPad Prism version 6 (GraphPad Software, La Jolla, CA). Raw RNA-Seq sequencing data has been uploaded to the National Center for Biotechnology Information's Sequence Read Archive (Accession no. PRJNA597441). To demonstrate the similarity across individual biological replicates, Principal Component Analysis (PCA) was performed using the Spotfire DecisionSite for Functional Genomics (DSFG) package (<http://spotfire.tibco.com/>).

Statistical Analysis

All statistical analyses were performed by GraphPad Prism version 6. Statistics of gene expression and sugar levels were determined using the Student's *t* test. The oocyst data were not normally distributed as determined by Shapiro-Wilk test. Thus, the Mann-Whitney test was used to determine the significance of oocyst intensities of dsRNA- treated mosquitoes.

Results

The phylogenetic analysis of glucose transporters in *Anopheles stephensi*

There are four genes annotated as glucose transporter, ASTE005839, ASTE003001, ASTE006385 and ASTE008063 in the database of *An. stephensi* (AsteS1.6). To investigate the relationships of these genes between *An. stephensi* and other organisms, a phylogenetic tree was constructed based on the amino

acid sequence of *Anopheles gambiae*, *Anopheles stephensi*, *Aedes aegypti*, *Drosophila melanogaster* and *Homo sapiens* by the maximum likelihood and Bayesian phylogenetic analyses (Fig. 1). The humans GLUT transporters can be divided into three classes, class 1 (GLUT1, GLUT2, GLUT3, GLUT4 and GLUT14), class 2 (GLUT5, GLUT7, GLUT9, and GLUT11) and class 3 (GLUT6, GLUT8, GLUT10 and GLUT12)[31, 32, 33, 34]. Due to the high similarity between *An. stephensi* ASTE005839, *Drosophila melanogaster* GLUT1 (FBpp0305693) and *Homo sapiens* GLUT1 (NP 006507.2), we named ASTE005839 *Asteglut1*. While ASTE008063 and ASTE006385 were categorized into GLUT- class3, so we named them *Asteglut3* and *Asteglut4*, respectively. ASTE003001 was not phylogenetically related to any GLUT-classes, so we named it *Asteglutx* (Fig 1).

Expression of *Astegluts* in *An. stephensi*

To determine the expression pattern of *Astegluts* in *An. stephensi*. We analyzed the expression levels of these genes in the head, salivary glands, midgut, ovary and carcass 24 hours before blood meal by qPCR, respectively. *Asteglut1*, *Asteglut3* and *Asteglut4* were mainly localized in the midgut tissue of *An. stephensi* (Fig. 2A, C, D). In addition to the midgut, *Asteglut1* and *Asteglut4* were also expressed in the head and salivary glands (Fig. 2A, D). *Asteglutx* was distributed in all five tissues (Fig. 2B). We next investigated the influence of parasite infection on the four *Astegluts* expression in the midgut. *Astegluts* were differentially regulated by *P. berghei* 24 hours post infection. (Fig. 2E). *P. berghei* infection significantly decreased the expression of *Asteglut1* and *Asteglut4*, while increased the expression of *Asteglutx* compared to those in normal blood feeding mosquitoes. No influence on *Asteglut3* expression was observed during parasite infection (Fig. 2E).

Knockdown of *Asteglut1* facilitates *Plasmodium berghei* infection in *An. stephensi*

To investigate the role of *Asteglut1*, *Asteglutx*, *Asteglut3* and *Asteglut4* in the capability of *An. stephensi* to transmit *P. berghei*, double-stranded RNA (dsRNA)-mediated silencing strategy was employed. The expression level of ds*Asteglut1*, ds*Asteglutx*, ds*Asteglut3* and ds*Asteglut4* was examined two days post dsRNA treatment. The expression level of these genes were significantly decreased by 57.8% ($P=0.02$), 40% ($P<0.0001$), 65% ($P=0.0002$) and 80% ($P=0.0013$) compared to *dsGFP* control, respectively (Fig 3A, B, C, D). However, only knockdown of *Asteglut1* significantly increased oocysts number of *P. berghei*. The ds*Asteglutx*, ds*Asteglut3* and ds*Asteglut4* treatments had no apparent effect on the intensity of *P. berghei* infection (Fig 3F, G, H). No significant difference of infection prevalence was observed between dsGFP and any ds*Asteglut* treated mosquitoes (Fig 3E, F, G, H). We next analyzed the knocking down specificity of *Asteglut1* and found this gene was knocked down specifically (Fig. 3I). Thus, the increasing susceptibility of *An. stephensi* to *P. berghei* infection was due to the knocking down of *Asteglut1*, instead of the compensatory effects of other *Astegluts* (Fig 3I).

Knockdown of *Asteglut1* significantly elevates glucose level in mosquito midgut

We next analyzed the influence of *Asteglut1* on sugar transportation in *An. stephensi*. The glucose and trehalose levels in the midgut and hemolymph of dsRNA treated mosquitoes were examined. The glucose level of *Asteglut1*-knockdown group was significantly higher than that in dsGFP controls 24 hours prior to blood-feeding (Fig. 4A). However, its level in hemolymph is comparable to that in dsGFP (Fig. 4C). There was no significant difference in sugar levels in the midgut or hemolymph either right before (0 hour) or 24 hours post blood-feeding (Fig 4). Knocking down of *Asteglut1* didn't change the level of trehalose either in the midgut or in hemolymph (Fig. 4B, D). Thus, *Asteglut1* might play a role in transportation of glucose but not trehalose in mosquito midgut.

Transcriptional analysis of *Asteglut1*-knockdown mosquitoes

To explore how *Asteglut1* regulated *P. berghei* infection, we performed a transcriptome analysis of mosquito's midgut treated with ds*Asteglut1* and dsGFP 24 hours post blood-meal, respectively. A total of 6 G PE clean sequences was generated by Illumina HiSeq 10 (Additional file 1: Table. S1). Principal Component Analysis (PCA) showed a clear separation between ds*Asteglut1* and dsGFP treatments (Additional file 2: Fig. S1). The Venn diagram shows that the expression of 10240 genes were overlapped in the two groups (Fig. 5A). A total 46 genes were differentially expressed (Fig. 5B, Additional file 3: Table. S2) with 26 up-regulated and 20 down-regulated. These differentially expressed genes were belong to the multiple functional clusters including cytoskeletal and structural, immunity, metabolism, proteolysis, redox, transport and unknown function (Fig. 5C).

Among the 'redox' functional cluster, five genes encoding cytochrome P450 (CYP450) were upregulated, indicating that the detoxification mechanism was activated in mosquitoes [35]. Gene encoding peroxiredoxin that controls cytokine-induced peroxide levels in mammalian cells was also significantly up-regulated, but the role of this gene in parasite control in mosquitoes is still unknown. [36]. We also observed DUOX that is involved in *Plasmodium* elimination significant down-regulated in ds*Asteglut1* treated mosquitoes [37]. It is highly possible that the reduction of DUOX expression might render mosquitoes more permissive to *P. berghei* infection.

The CLIP family are involved in the melanization of *P. berghei* in *An. gambiae* [38]. Two CLIP genes, *clip2* and *clip9*, were significantly down regulated in ds*Asteglut1* treated mosquitoes compared to dsGFP ones, while *clipb3* was upregulated [38, 39]. We next examined whether the increasing parasite infection could be due to the dysregulation in mosquito melanization. Midguts of mosquitoes treated with dsRNA 8 days post infection were collected and melanization was visualized microscopically. We found that the number of melanized ookinete increased with the number of oocysts (Fig. 5D). Thus there was no significant difference in the melanization rate between ds*Asteglut1* and dsGFP group.

Five immune related genes were differentially regulated. *Caudal*, the negative regulator of Imd pathway was significantly up-regulated [40], while the peptidoglycan recognition proteins, *pgrp-la*, *-lc*, *-ld*, and the antimicrobial peptides, *defensin* were significantly down-regulated [25, 40, 41, 42, 43]. These results indicate that AsteGlut1 might control parasite infection by regulating mosquito immune responses.

Discussion

The glucose transporter family, functionally conserved from insects to mammals, is responsible for the transportation of glucose across the cell membrane [44]. In mammals, GLUT1 is one of the earliest cloned membrane transporters and has been extensively investigated in the past half century [45]. It is ubiquitously expressed in the skeletal, muscle, heart, and other tissues, but predominantly functions in erythrocytes and blood–brain barrier [33, 45, 46]. In *An. stephensi*, *Plasmodium* undergoes a drastic reduction during the early stage of their infection in mosquitoes. In the entire *Plasmodium* life cycle (in both human and mosquito hosts), parasite numbers are the lowest at oocyst stage and then quickly expand with thousands of sporozoites produced per oocyst [47]. For this reason, we focus on the interactions between the midgut stages of parasite and mosquitoes aiming to find possible target for vector control. We identify 4 *glut* genes, *Asteglut1*, *Asteglut3*, *Asteglutx* and *Asteglut4*. They have distinct expression patterns, suggesting their potential different roles in glucose transportation. Knockdown of *Asteglut1* increases the glucose level in midgut, suggesting its role in maintaining the homeostasis of intestinal glucose. However, we did not observe significant changes of glucose and trehalose level in the hemolymph. It is highly possible that sugar level in hemolymph is controlled by multiple factors and functional redundancy exists between members of the Asteglut family.

In addition, we also find that knocking down *Asteglut1* influences mosquito's susceptibility to *P. berghei* infection. In agreement with our findings, GLUT1 is involved in the regulation of pathogen infection in mammals. GLUT1 is a natural receptor of T-lymphotropic virus (HTLV) that facilitates the invasion of HTLV in human cells. [48]. GLUT1 is also involved in the regulation of CD4⁺ T cell function in human. Knocking out GLUT1 in CD4⁺ T cell reduces glucose uptake and glycolysis, and also impairs the growth, proliferation, survival and differentiation of these cells [49]. In plant, the expression of sugar transporter (SWEET) is induced by bacteria and fungi infection. Knockout of SWEET limits the growth of these pathogens [50]. In *An. stephensi*, invasion of *P. berghei* into salivary glands induces the expression of glucose transporter, *AGAP007752*. Its knockdown decreased the number of sporozoites in mosquito salivary glands. [19, 20, 21].

Asteglut1 help to defend against *P. berghei* might through regulating midgut glucose level. The accumulation of glucose in the midgut when *Asteglut1* is knocked down might change multiple biological processes, which effect synergistically to increase parasite infection. Our transcriptome analysis reveals that a considerable number of up-regulated genes are cytochrome P450, which is the family that responsible for the detoxification [51]. The upregulation of cytochrome P450 genes in ds*Asteglut1* treated mosquitoes indicate that these mosquitoes might suffer more toxicity than that in control [51, 52]. In addition to catabolizing xenobiotics, the cytochrome P450 also involves in the anabolism and catabolism

of of hormones [53]. For example, cytochrome P450s are involved in the biosynthesis of 20-hydroxyecdysone (20E) from cholesterol [54]. The steroid hormone 20E not only promotes oogenesis in mosquitoes, but also facilitates *Plasmodium* infection [55]. Thus, the elevated levels of P450 genes expression might be responsible for the increased parasite infection.

The role of CLIP family members function as either activators or suppressors of melanization that is responsible for elimination of *P. berghei* in *An. gambiae* [38]. Although 3 *clips* genes are differentially regulated in dsAsteglut1 treated mosquitoes, we don't observe any difference of melanization rates between dsGFP and dsAsteglut1 treated mosquitoes. This result suggested that these CLIPs might function differently from the classical CLIPS. Further investigation of their function is needed in the future.

We also notice the significant induction of *caudal*, and reduction of *pgrps*, *pgrp-la*, *-lc*, *-ld*, and the antimicrobial peptides, *defensin* in dsAsteglut1 mosquitoes, suggesting that Asteglut1 might be involved in the regulation of immune responses [25, 40, 56]. PGRP-LA is a receptor of mosquito immune deficiency pathway (Imd) [41]. It helps to control the homeostasis of gut microbiota and parasite infection in *An. stephensi* [57]. PGRP-LC is the primary receptor of Imd pathway. Silencing PGRP-LC blocks the synthesis of downstream immune effectors, which in turn increases parasites infection [42]. Different from PGRP-LA and LC, PGRP-LD is a negative regulator of immune signaling pathway. However, knockdown of PGRP-LD similarly increased susceptibility of *An. stephensi* to *P. berghei* infection through compromised peritrophic matrix integrity. The compromised peritrophic matrix structure results from the reduction of gut microbiota in the absence of protection by PGRP-LD [25]. Thus the downregulation of *pgrp-la*, *-lc* and *-ld* all lead to the increasing susceptibility of *Anopheles* mosquito to *Plasmodium* infection [25, 42, 57]. However, how Asteglut1 regulates Imd pathway needs to be investigated in the future.

Conclusion

In summary, we identify 4 GLUT members in *An. stephensi* and find Asteglut1 participates in the defense against *P. berghei* infection. The regulation of Asteglut1 on vector competence might through modulating multiple biological processes, especially detoxification and immunity (Fig 6). Our findings would pave the way for further understanding how sugar transporter regulate vector-parasite interaction and will help to explore potential new targets for vector control.

Additional File Information

Additional file 1: Table S1 Summary of RNA-sequencing data generated using Illumina HiSeq platform.

Additional file 2: Table S2. List of significantly differentially expressed genes.

Additional file 3: Fig S1. Principal Component Analysis (PCA) showing similarities between transcriptome profiles produced by RNA-Seq.

Abbreviations

Asteglut: glucose transporter in *Anopheles stephensi*; CYP450: cytochrome P450; DUOX: dual oxidase; CLIP: class of serine proteases.

Declarations

Acknowledgements

Not applicable.

Ethics approval and consent to participate

All animals were handled strictly in accordance with the guidelines of the Care and Use of Laboratory Animals of the National Institutes of Health and the Office of Laboratory Animal Welfare, China. The research protocol was approved by the Institutional animal care and use committee, Department of Laboratory Animal Science, Fudan University, China.

Consent for publication

Not applicable.

Availability of data and materials

All data generated or analyzed during this study are included in this published article and its additional files.

Competing interests

The authors declare that they have no competing interests.

Funding

This research was supported by National Natural Science Foundation of China (31822051, U1902211) (<https://isisn.nsf.gov.cn/egrantweb/>) and National Institutes of Health Grant (R01AI129819) (<https://grants.nih.gov/grants>).

Authors' contributions

MF performed the experiments, drafted the manuscript and data analysis. MF and JW revised the manuscript. All authors read and approved the final manuscript.

Author details

References

1. WHO. World Malaria Report 2018. Geneva: World Health Organization. <https://www.who.int/malaria/publications/world-malaria-report-2018/en/>. Accessed 10 May 2019. 2018.
2. de Koning-Ward TF, Dixon MW, Tilley L, Gilson PR. *Plasmodium* species: master renovators of their host cells. *Nature reviews Microbiology*. 2016;14:494-507.
3. Bennink S, Kiesow MJ, Pradel G. The development of malaria parasites in the mosquito midgut. *Cellular microbiology*. 2016;18:905-18.
4. Martin SK, Jett M, Schneider I. Correlation of phosphoinositide hydrolysis with exflagellation in the malaria microgametocyte. *The Journal of parasitology*. 1994;371-8.
5. Brancucci NMB, Gerdt JP, Wang C, De Niz M, Philip N, Adapa SR, et al. Lysophosphatidylcholine Regulates Sexual Stage Differentiation in the Human Malaria Parasite *Plasmodium falciparum*. *Cell*. 2017;171:1532-44.e15.
6. Gu W, Müller G, Schlein Y, Novak RJ, Beier JC. Natural plant sugar sources of *Anopheles* mosquitoes strongly impact malaria transmission potential. *PloS one*. 2011;6:e15996.
7. Hien DF, Dabire KR. Plant-mediated effects on mosquito capacity to transmit human malaria. *PLoS pathogens*. 2016;12:e1005773.
8. Manda H, Gouagna LC, Foster WA, Jackson RR, Beier JC, Githure JI, et al. Effect of discriminative plant-sugar feeding on the survival and fecundity of *Anopheles gambiae*. *Malar J*. 2007;6:113.
9. Nyasembe VO, Teal PEA, Mukabana WR, Tumlinson JH, Torto B. Behavioural response of the malaria vector *Anopheles gambiae* to host plant volatiles and synthetic blends. *Parasites & vectors*. 2012;5:234.
10. Okech BA, Gouagna LC, Kabiru EW, Beier JC, Yan G, Githure JI. Influence of age and previous diet of *Anopheles gambiae* on the infectivity of natural *Plasmodium falciparum* gametocytes from human volunteers. *Journal of Insect Science*. 2004;4:33.
11. Reyes-DelaTorre A, Teresa M, Rafael J. Carbohydrates-comprehensive studies on glycobiology and glycotecchnology. vol. 14; 2012.
12. Mack SR, Samuels S, Vanderberg JP. Hemolymph of *Anopheles stephensi* from Noninfected and *Plasmodium berghei*-Infected Mosquitoes. 3. Carbohydrates. *The Journal of Parasitology*. 1979;65:217-21.
13. Liu K, Dong Y, Huang Y, Rasgon JL, Agre P. Impact of trehalose transporter knockdown on *Anopheles gambiae* stress adaptation and susceptibility to *Plasmodium falciparum* infection. *Proceedings of the National Academy of Sciences of the United States of America*. 2013;110:17504-9.

14. Kirk K, Horner HA, Kirk J. Glucose uptake in *Plasmodium falciparum*-infected erythrocytes is an equilibrative not an active process. *Molecular and biochemical parasitology*. 1996;82:195-205.
15. Yuval B, Holliday-Hanson ML, Washing RK. Energy budget of swarming male mosquitoes. *Ecological Entomology*. 1994;19:74-8.
16. Meireles P, Sales-Dias J, Andrade CM, Mello-Vieira J, Mancio-Silva L, Simas JP, et al. GLUT1-mediated glucose uptake plays a crucial role during *Plasmodium* hepatic infection. *Cellular microbiology*. 2016;19:e12646.
17. Hellwig B, Joost HG. Differentiation of erythrocyte-(GLUT1), liver-(GLUT2), and adipocyte-type (GLUT4) glucose transporters by binding of the inhibitory ligands cytochalasin B, forskolin, dipyrindamole, and isobutylmethylxanthine. *Molecular pharmacology*. 1991;40:383-9.
18. Woodrow CJ, Burchmore RJ, Krishna S. Hexose permeation pathways in *Plasmodium falciparum*-infected erythrocytes. *Proceedings of the National Academy of Sciences of the United States of America*. 2000;97:9931-6.
19. Couto J, Antunes S, Ferrolho J, de La Fuente J, Domingos A. Reduction of Mosquito survival in mice vaccinated with *Anopheles stephensi* glucose transporter. *BioMed research international*. 2017;2017:e428186.
20. Pinheiro-Silva R, Lara B, Pedro Coelho L, Cabezas-Cruz A, Valdés JJ, do Rosário V, et al. Gene expression changes in the salivary glands of *Anopheles coluzzii* elicited by *Plasmodium berghei* infection. *Parasites & vectors*. 2015;8:485.
21. Couto J, Antunes S, Pinheiro-Silva R, do Rosario V, de la Fuente J, Domingos A. Solute carriers affect *Anopheles stephensi* survival and *Plasmodium berghei* infection in the salivary glands. *Scientific Reports*. 2017;7:6141.
22. Sinden RE. Infection of mosquitoes with rodent malaria. *The molecular biology of insect disease vectors*: Springer; 1997. p. 67-91.
23. Franke-Fayard B, Trueman H, Ramesar J, Mendoza J, van der Keur M, van der Linden R, et al. A *Plasmodium berghei* reference line that constitutively expresses GFP at a high level throughout the complete life cycle. *Molecular and biochemical parasitology*. 2004;137:23-33.
24. Kumar S, Stecher G, Li M, Knyaz C, Tamura K. MEGA X: Molecular Evolutionary Genetics Analysis across Computing Platforms. *Mol Biol Evol*. 2018;35:1547-9.
25. Song X, Wang M, Dong L, Zhu H, Wang J. PGRP-LD mediates *A. stephensi* vector competency by regulating homeostasis of microbiota-induced peritrophic matrix synthesis. *PLoS pathogens*. 2018;14:e1006899.
26. Song W, Ren D, Li W, Jiang L, Cho KW, Huang P, et al. SH2B Regulation of Growth, Metabolism, and Longevity in Both Insects and Mammals. *Cell Metabolism*. 2010;11:427-37.
27. Holmes DS, Bonner J. Preparation, molecular weight, base composition, and secondary structure of giant nuclear ribonucleic acid. *Biochemistry*. 1973;12:2330-8.
28. Li B, Dewey CN. RSEM: accurate transcript quantification from RNA-Seq data with or without a reference genome. *BMC Bioinformatics*. 2011;12:323.

29. Robinson MD, McCarthy DJ, Smyth GK. edgeR: a Bioconductor package for differential expression analysis of digital gene expression data. *Bioinformatics*. 2010;26:139-40.
30. Chen C, Xia R, Chen H, He Y. TBtools, a Toolkit for Biologists integrating various HTS-data handling tools with a user-friendly interface. *bioRxiv*. 2018:289660.
31. Deng D, Yan N. GLUT, SGLT, and SWEET: Structural and mechanistic investigations of the glucose transporters. *Protein science : a publication of the Protein Society*. 2016;25:546-58.
32. Thorens B, Mueckler M. Glucose transporters in the 21st Century. *American journal of physiology Endocrinology and metabolism*. 2010;298:E141-5.
33. Mueckler M, Thorens B. The SLC2 (GLUT) family of membrane transporters. *Mol Aspects Med*. 2013;34:121-38.
34. Chen LQ, Cheung LS, Feng L, Tanner W, Frommer WB. Transport of sugars. *Annual review of biochemistry*. 2015;84:865-94.
35. Ranson H, Nikou D, Hutchinson M, Wang X, Roth C, Hemingway J, et al. Molecular analysis of multiple cytochrome P450 genes from the malaria vector, *Anopheles gambiae*. *Insect molecular biology*. 2002;11:409-18.
36. Rhee SG, Chae HZ, Kim K. Peroxiredoxins: a historical overview and speculative preview of novel mechanisms and emerging concepts in cell signaling. *Free Radical Biology and Medicine*. 2005;38:1543-52.
37. Cirimotich CM, Dong Y, Garver LS, Sim S, Dimopoulos G. Mosquito immune defenses against *Plasmodium* infection. *Developmental & Comparative Immunology*. 2010;34:387-95.
38. Barillas-Mury C. CLIP proteases and *Plasmodium* melanization in *Anopheles gambiae*. *Trends in parasitology*. 2007;23:297-9.
39. Gorman MJ, Paskewitz SM. Serine proteases as mediators of mosquito immune responses. *Insect biochemistry and molecular biology*. 2001;31:257-62.
40. Clayton AM, Cirimotich CM, Dong Y, Dimopoulos G. Caudal is a negative regulator of the *Anopheles* IMD pathway that controls resistance to *Plasmodium falciparum* infection. *Developmental and comparative immunology*. 2013;39:323-32.
41. Gendrin M, Turlure F, Rodgers FH, Cohuet A, Morlais I, Christophides GK. The Peptidoglycan Recognition Proteins PGRPLA and PGRPLB Regulate *Anopheles* Immunity to Bacteria and Affect Infection by *Plasmodium*. *J Innate Immun*. 2017;9:333-42.
42. Meister S, Agianian B, Turlure F, Relógio A, Morlais I, Kafatos FC, et al. *Anopheles gambiae* PGRPLC-mediated defense against bacteria modulates infections with malaria parasites. *PLoS pathogens*. 2009;5:e1000542.
43. Richman A, Bulet P, Hetru C, Barillas-Mury C, Hoffmann J, Kafatos F. Inducible immune factors of the vector mosquito *Anopheles gambiae*: biochemical purification of a defensin antibacterial peptide and molecular cloning of preprodefensin cDNA. *Insect molecular biology*. 1996;5:203-10.
44. Mueckler M. Facilitative glucose transporters. *Eur J Biochem*. 1994;219:713-25.

45. Mueckler M, Caruso C, Baldwin SA, Panico M, Blench I, Morris HR, et al. Sequence and structure of a human glucose transporter. *Science*. 1985;229:941-5.
46. Keller SR, Davis AC, Clairmont KB. Mice deficient in the insulin-regulated membrane aminopeptidase show substantial decreases in glucose transporter GLUT4 levels but maintain normal glucose homeostasis. *Journal of Biological Chemistry*. 2002;277:17677-86.
47. Smith RC, Vega-Rodriguez J, Jacobs-Lorena M. The *Plasmodium* bottleneck: malaria parasite losses in the mosquito vector. 2014;109:644-61.
48. Manel N, Kim FJ, Kinet S, Taylor N, Sitbon M, Battini J-L. The ubiquitous glucose transporter GLUT-1 is a receptor for HTLV. *Cell*. 2003;115:449-59.
49. Macintyre AN, Gerriets VA, Nichols AG, Michalek RD, Rudolph MC, Deoliveira D, et al. The glucose transporter Glut1 is selectively essential for CD4 T cell activation and effector function. *Cell metabolism*. 2014;20:61-72.
50. Chen L-Q, Hou B-H, Lalonde S, Takanaga H, Hartung ML, Qu X-Q, et al. Sugar transporters for intercellular exchange and nutrition of pathogens. *Nature*. 2010;468:527-32.
51. Strode C, Wondji CS, David J-P, Hawkes NJ, Lumjuan N, Nelson DR, et al. Genomic analysis of detoxification genes in the mosquito *Aedes aegypti*. *Insect biochemistry and molecular biology*. 2008;38:113-23.
52. Félix RC, Müller P, Ribeiro V, Ranson H, Silveira H. *Plasmodium* infection alters *Anopheles gambiae* detoxification gene expression. *BMC genomics*. 2010;11:312.
53. Scott JG. Insect cytochrome P450s: thinking beyond detoxification. *Recent advances in insect physiology, toxicology and molecular biology*. 2008;1:17-124.
54. Rewitz KF, O'Connor MB, Gilbert LI. Molecular evolution of the insect Halloween family of cytochrome P450s: phylogeny, gene organization and functional conservation. *Insect biochemistry and molecular biology*. 2007;37:741-53.
55. Werling K, Shaw WR, Itoe MA, Westervelt KA, Marcenac P, Paton DG, et al. Steroid hormone function controls non-competitive *Plasmodium* development in *Anopheles*. *Cell*. 2019;177:315-25. e14.
56. Yassine H, Osta MA. *Anopheles gambiae* innate immunity. *Cellular microbiology*. 2010;12:1-9.
57. Gao L, Song X, Wang J. Gut microbiota is essential in PGRP-LA regulated immune protection against *Plasmodium berghei* infection. *Parasites & vectors*. 2020;13:3.

Figures

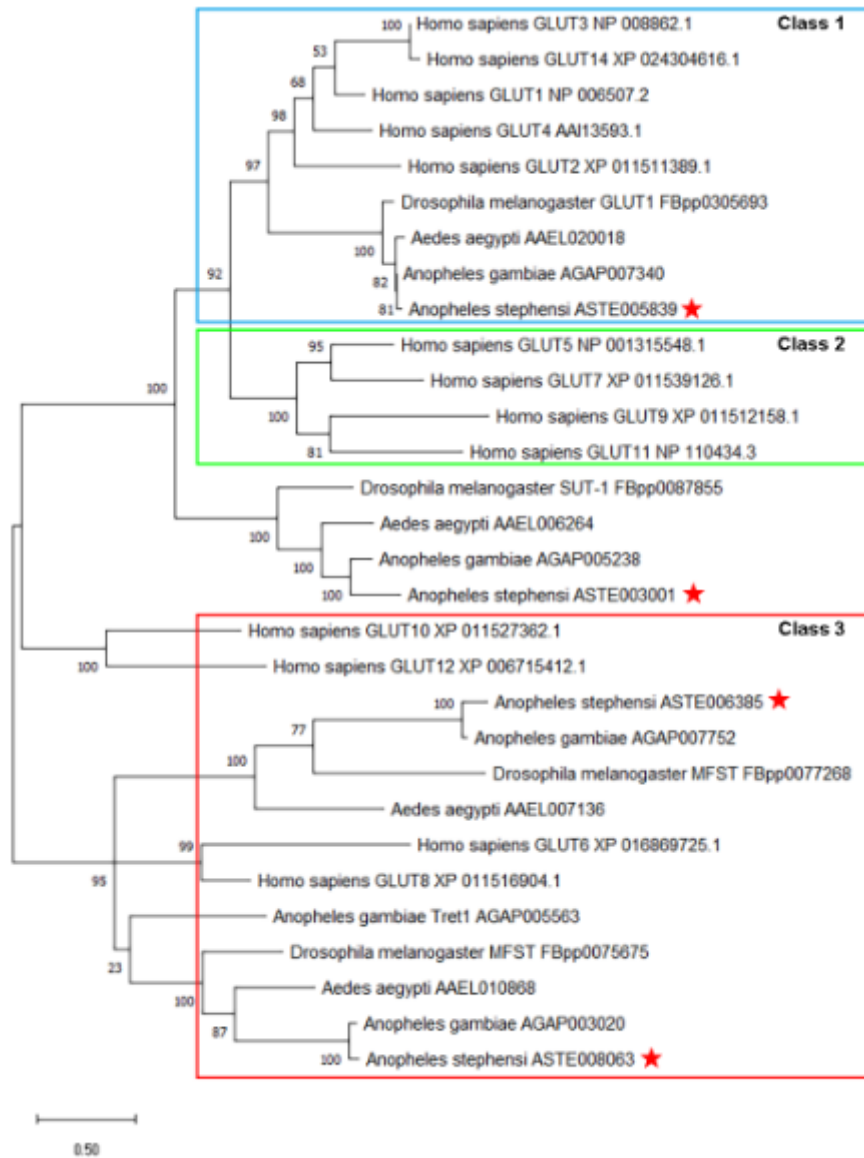


Figure 1

Phylogenetic analysis of glucose transporters (GLUTs) in *An. stephensi* and other organisms. The genes involved in this study were marked with red stars. The family of GLUT transporters known in humans are divided into three classes, class 1 (blue box), class 2 (green box) and class 3 (red box).

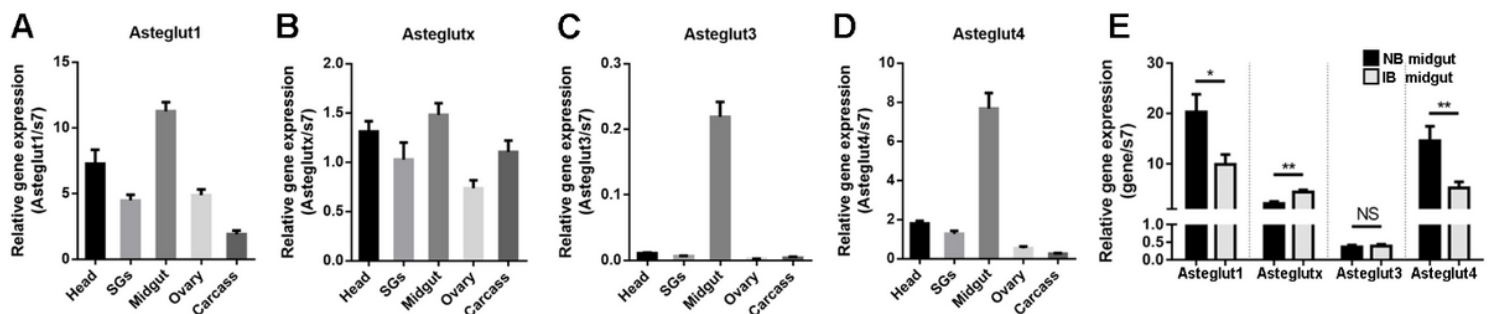


Figure 2

Expression patterns of Asteglut1, Asteglutx, Asteglut3 and Asteglut4 in *An. stephensi*. A, B, C, D Relative gene expression of Asteglut1, Asteglutx, Asteglut3 and Asteglut4 in the head, salivary glands (SGs), midgut, ovary and carcass 24 hours before blood meal by qPCR, respectively. E Relative gene expression of Asteglut1, Asteglutx, Asteglut3 and Asteglut4 in the midgut 24 hours post normal (NB) or infectious blood (IB) meal. Error bars indicate standard error of the mean (n = 5). Results from one of two independent experiments are shown.

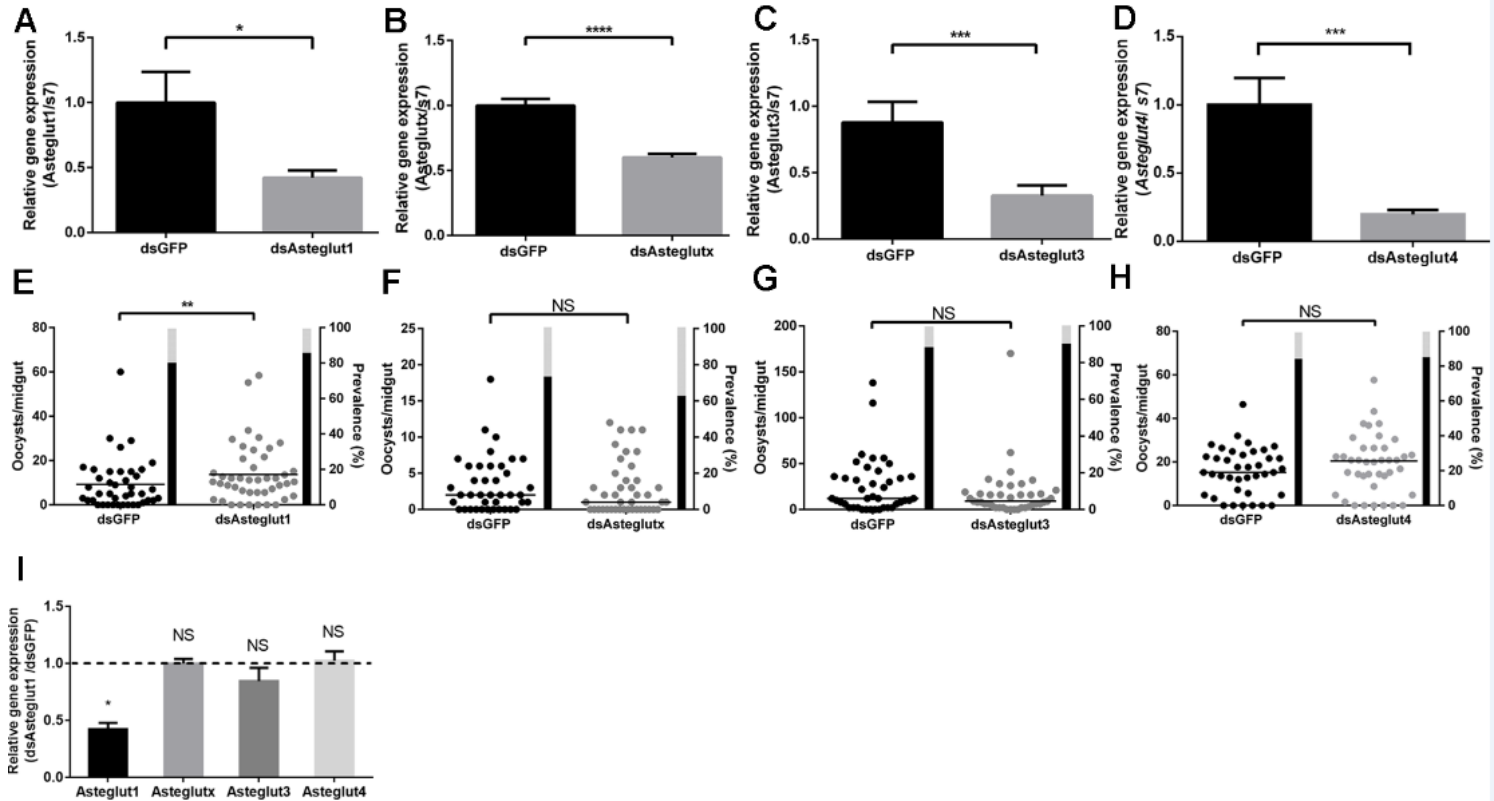


Figure 3

Knocking down of Asteglut1, Asteglutx, Asteglut3 and Asteglut4 in *An. stephensi* and *P. berghei* oocysts in dsRNA treated mosquitoes. A, B, C, D Asteglut1, Asteglutx, Asteglut3, Asteglut4 knockdown efficiency. Relative expression level of Asteglut1, Asteglutx, Asteglut3, Asteglut4 were normalized to that in dsGFP controls. Ribosomal gene s7 used as an internal control. Error bars indicate standard error of the mean (n=10). Results from one of three independent experiments are shown. Significance was determined by Student's -t- test. E, F, G, H Median number of oocyst in dsRNA treated mosquitoes. Each dot represents an individual mosquito and horizontal lines represent the medians. Results from one of three independent experiments are shown. Significance was determined by Mann-Whitney test. I Specificity of dsAsteglut1 treatment. Relative expression level of Asteglutx, Asteglut3, Asteglut4 in dsAsteglut1 mosquitoes were normalized to that in dsGFPs. Error bars indicate standard error of the mean (n=10). Results from one of three independent experiments are shown. Significance was shown by Student's -t- test. NS, no significance, *p < 0.05, **p < 0.01, ***p < 0.001, ****p < 0.0001.

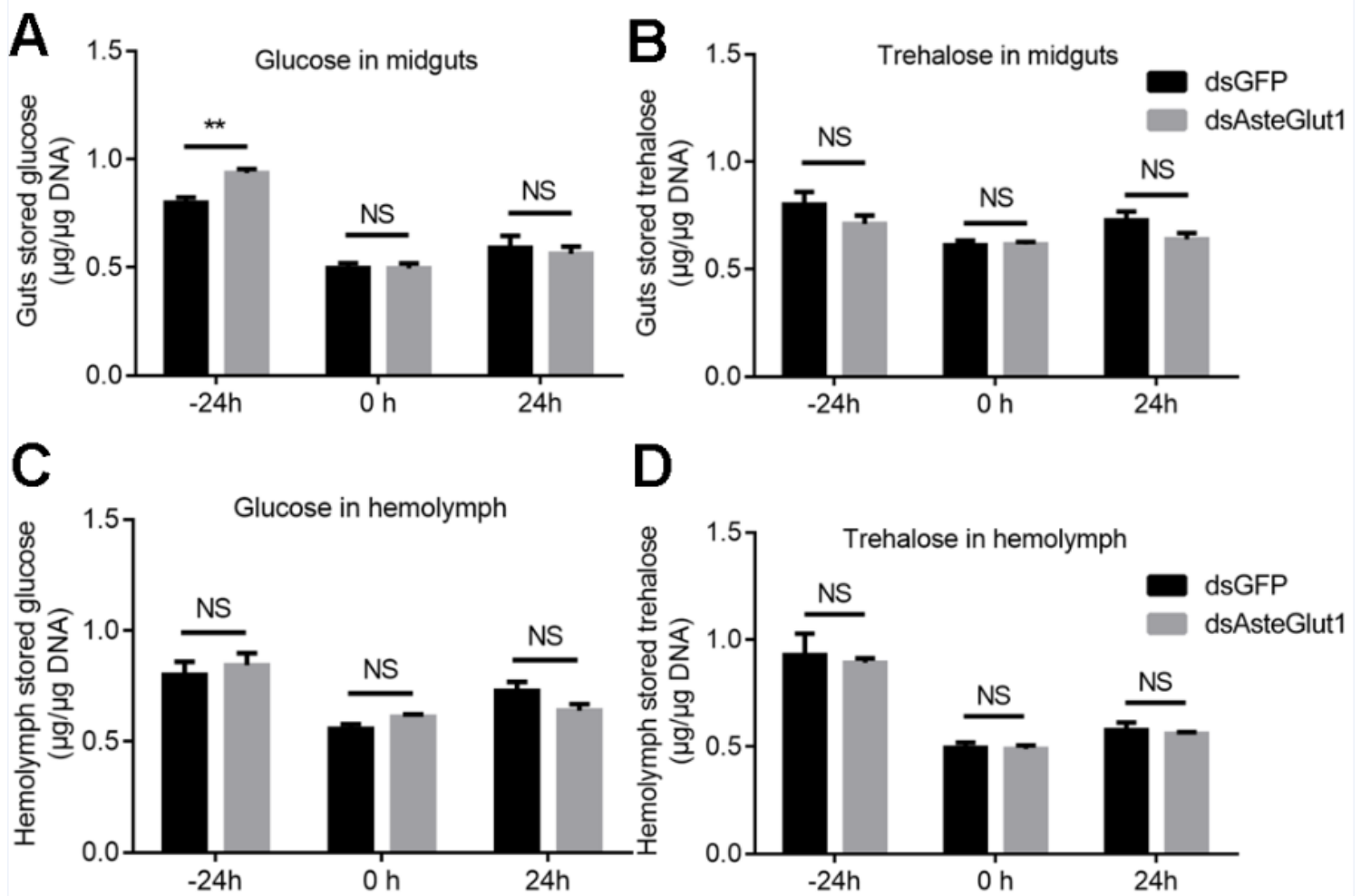


Figure 4

Knocking down of Asteglut1 significantly elevates the level of glucose in mosquito midgut. The relative concentration of glucose (A and C) and trehalose (B and D) level in midgut and hemolymph of GFP or Asteglut1 dsRNA- injected *An. stephensi* 24 hours prior to (-24h), right before (0 h) and 24 hours post (24h) feeding with blood meal respectively. Sugar concentrations were normalized to genomic DNA extracted from midgut or hemolymph cells. Data represent mean \pm SEM, significance was determined by Student's *t*-test. NS, no significance, * $p < 0.05$, ** $p < 0.01$, *** $p < 0.001$, **** $p < 0.0001$.

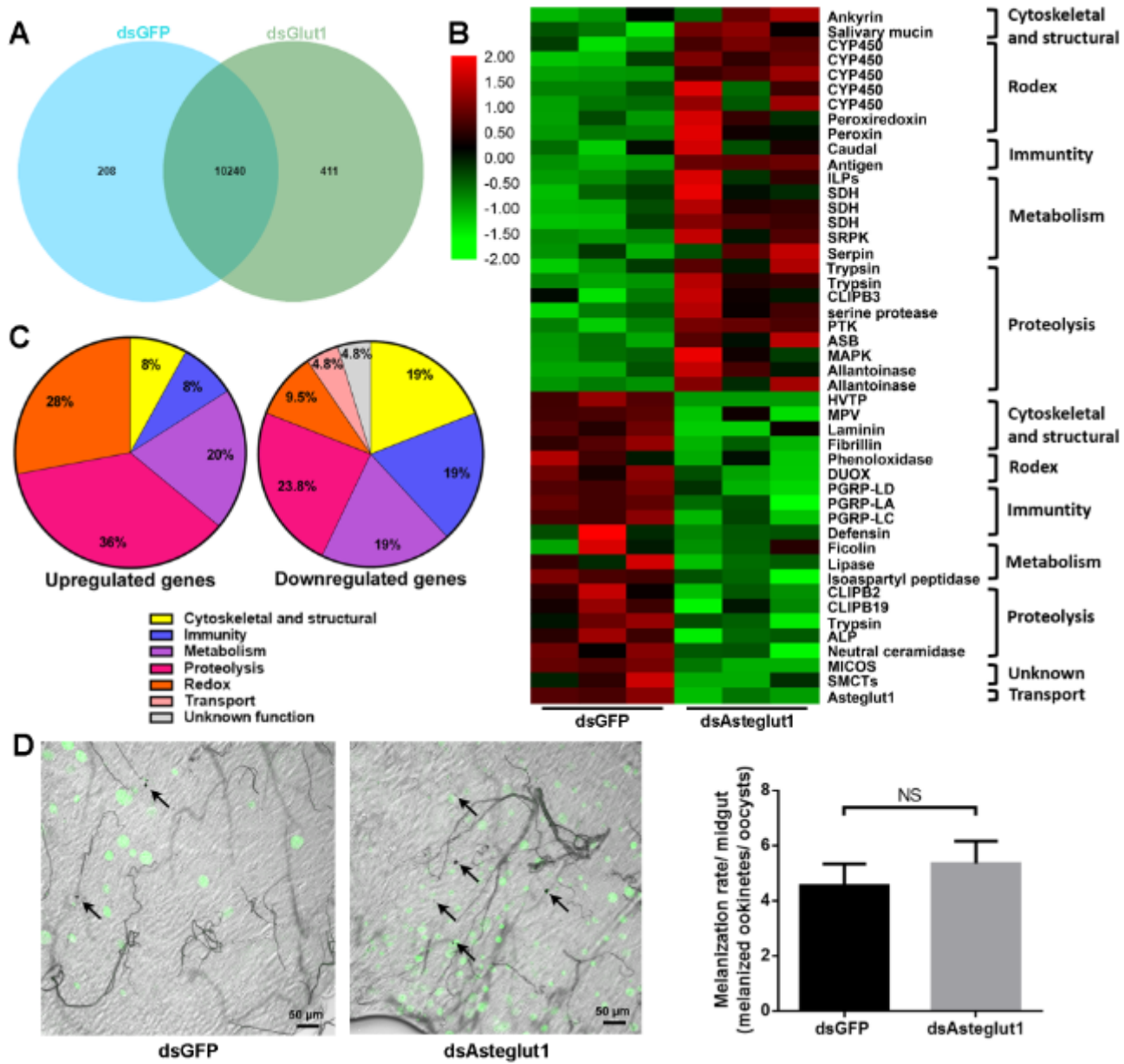


Figure 5

Transcriptional response in *An. stephensi* midguts infected with *P. berghei*. A Venn diagram showing the overlap of genes between dsGFP and dsAsteglut1 treated groups. B Heatmap representing the differentially expressed genes based on Gene Ontology assignments in *An. stephensi* midguts infected with *P. berghei*. Upregulated genes are shown in red; downregulated genes are shown in green ($p < 0.05$; fold change > 2). C Summary of the distribution of upregulated genes (left side) and downregulated genes (right side). D Left panel, live *Plasmodium* oocysts (green) and melanized ookinetes (black spots) in midguts of dsGFP and dsAsteglut1 treated mosquitoes. Right panel, melanization rate, the melanization rate was calculated by the ratio of the number of melanized ookinetes to the number of live *Plasmodium* oocysts observed per midgut.

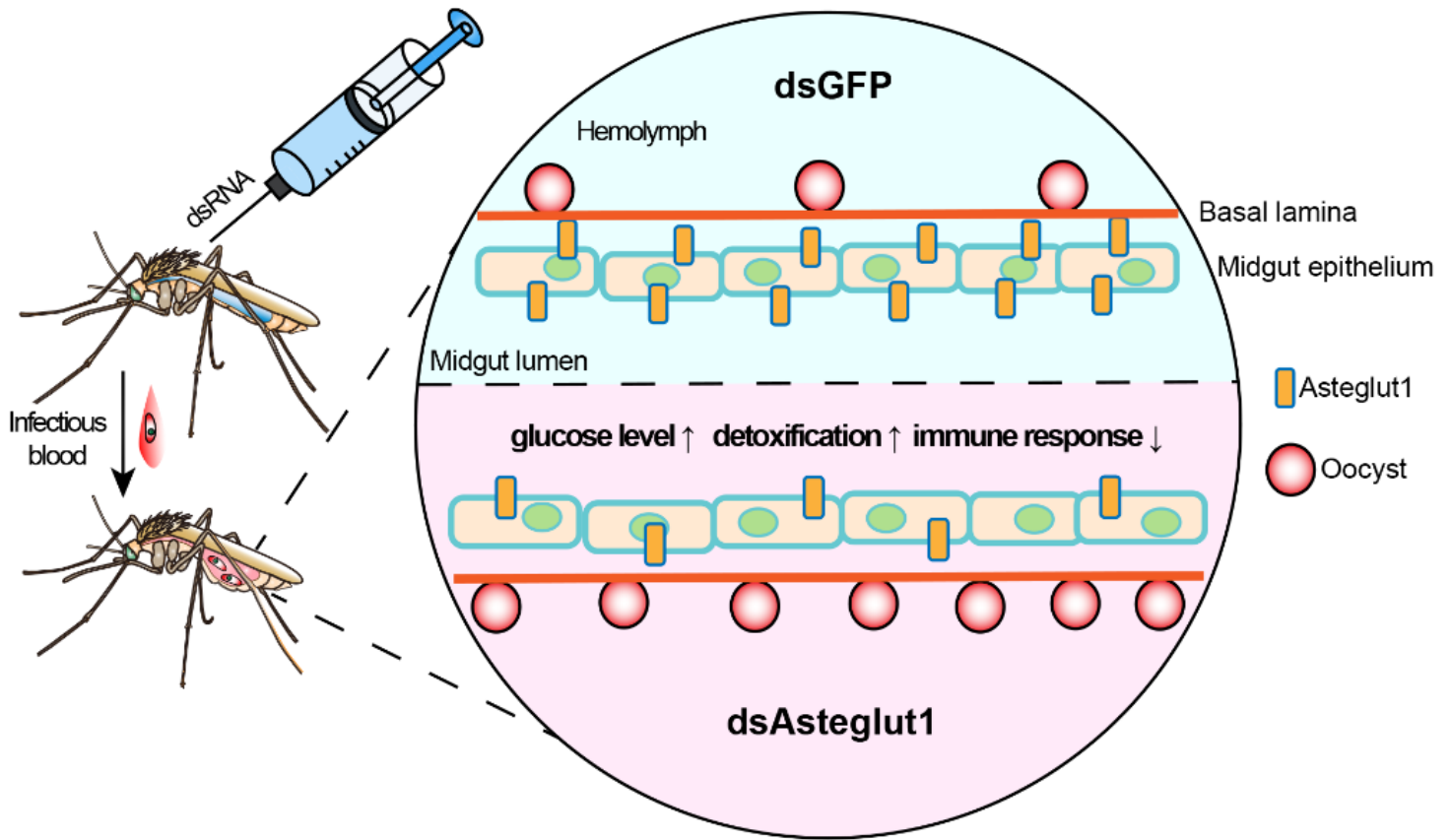


Figure 6

Model of influence of dsAsteglut1 in *An. stephensi*. Abrogation of Asteglut1 significantly increased the susceptibility of *An. stephensi* to *Plasmodium berghei* infection. The regulation of Asteglut1 on vector competence might through modulating multiple biological processes, including detoxification and immunity.

Supplementary Files

This is a list of supplementary files associated with this preprint. Click to download.

- [FigS1.tif](#)
- [GraphicalAbstract.tif](#)
- [TableS1.docx](#)
- [TableS2.xlsx](#)